Normal function of HERG K^+ channels expressed in HEK293 cells requires basal protein kinase B activity

Yiqiang Zhang[a,b], Huizhen Wang[a,b], Jingxiong Wang[a,b], Hong Han[a], Stanley Nattel[a,c,d], Zhiguo Wang[a,b,*]

[a] *Research Center, Montreal Heart Institute, Montreal, QC, Canada H1T 1C8*
[b] *Department of Medicine, University of Montreal, Montreal, QC, Canada H3C 3J7*
[c] *Department of Pharmacology, University of Montreal, Montreal, QC, Canada H3C 3J7*
[d] *Department of Pharmacology and Therapeutics, McGill University, Montreal, QC, Canada H3A 2T5*

Received 19 September 2002; revised 2 December 2002; accepted 2 December 2002

First published online 13 December 2002

Edited by Maurice Montal

Abstract The potential role of protein kinase B (PKB), a serine/threonine protein kinase, in regulating HERG (human *ether-a-go-go* related gene) K^+ channel function was investigated. Wortmannin (a phosphoinositide 3-kinase (PI3K) inhibitor) caused ~30% reduction of HERG current (I_{HERG}) stably expressed in HEK293 cells. Transient transfection with the constitutively active PI3K in HERG-expressing HEK293 cells slightly increased (~7%) I_{HERG} while a dominant negative PI3K significantly reduced I_{HERG} (~25%) relative to results in vehicle-transfected cells. I_{HERG} was ~35% greater in cells transfected with the constitutively activated PKB (caPKB), whereas it was ~47% smaller in cells transfected with dominant negative PKB (dnPKB). Basal activation of PKB was detected by immunocytochemistry. PKB activity was significantly enhanced in caPKB-transfected cells and nearly abolished in dnPKB-transfected cells. We conclude that normal HERG function in HEK293 cells requires basal activity of PKB. Our data represent the first evidence that PKB phosphorylation regulates K^+ channels.

Key words: Human *ether-a-go-go* related gene; Protein kinase B; Phosphoinositide 3-kinase; Wortmannin; Patch-clamp; Immunocytochemistry

1. Introduction

Protein kinase B (PKB), a downstream target of phosphoinositide 3-kinase (PI3K), is a serine/threonine (Ser/Thr) protein kinase first identified several years ago [1,2]. The cDNA sequence of PKB displays high sequence homology to both the protein kinase C and the protein kinase A family of Ser/Thr kinases. It was therefore termed protein kinase B (PKB) [1,2]. PKB can be activated by a wide variety of stimuli in a PI3K-dependent or -independent manner [3,4]. The fungal metabolite wortmannin (WMN) is a potent inhibitor of kinase activities of class I PI3K, with an IC_{50} in the range of 1–10 nM [5]. By inhibiting PI3K, WMN can prevent PI3K-dependent activation of PKB and it has been widely used to study the physiological role of the PI3K/PKB signaling pathway in various cellular processes.

It is well established that PKA and PKC can both regulate ion channel function by Ser/Thr phosphorylation of channel proteins, providing an important mechanism for regulation of cell function. In contrast, the potential role of PKB in modulating ion channel function has been largely ignored. Only recently has the PI3K/PKB pathway been found to be involved in the regulation of some ion channels, for example, the potentiation of L-type Ca^{2+} current and M-current in neurons [6,7], enhancement of Cl^- currents in rat hepatoma cells [8], and up-regulation of several *Shaker*-type K^+ channels in human embryonic kidney cell line [9]. It is believed that modulation of these ion channels contributes to regulation by PI3K/PKB of cell survival, cell growth, cell column and other cell functions. Among these studies, however, only the work reported by Blair et al. [6] demonstrated that the modulation of the L-channel was PKB-dependent.

HERG (human *ether-a-go-go* related gene) encodes the rapid component of delayed rectifier K^+ current in the heart, and HERG dysfunction is known to account for both inherited and acquired long Q-T syndrome [10], a potentially lethal arrhythmia. Recent studies have revealed widespread distribution of HERG in various tissues and cells outside the heart, including neurons [11,12], pancreatic β-cells [13], and a variety of tumor cells [14,15], where in addition to its cardiac electrophysiological role, HERG may also participate in the regulation of cell growth and death [16]. The HERG protein contains two putative consensus sequence motifs for PKB phosphorylation located at S890 and S331 [4,17,18]. Although HERG has been found to be a target for PKA phosphorylation [19–21] and probably also for PKC [22,23], it is unknown whether it is also a substrate for PKB. The present study was therefore undertaken to define the potential regulation of HERG channel function by PKB.

2. Materials and methods

2.1. Cell culture

HEK293 cells stably expressing HERG (a kind gift from Drs. Z Zhou and C. January) [24] were seeded in a 25 cm^2 cell culture flask

*Corresponding author. Fax: (1)-514-376 4452.
E-mail address: wangz@icm.umontreal.ca (Z. Wang).

Abbreviations: Bis, bisindolylmaleimide; *HERG*, human *ether-a-go-go* related gene; HERG, K^+ channel protein encoded by *HERG*; I_{HERG}, current expressed by HERG; PKB, protein kinase B; caPKB, constitutively active PKB; dnPKB, dominant negative PKB; PI3K, phosphoinositide 3-kinase; caPI3K, constitutively active PI3K; dnPI3K, dominant negative PI3K; WMN, wortmannin

0014-5793/02/$22.00 © 2002 Published by Elsevier Science B.V. on behalf of the Federation of European Biochemical Societies.
doi:10.1016/S0014-5793(02)03804-8

and grown in Dulbecco's modified Eagle's medium (DMEM, Life Technologies) supplemented with 10% heat-inactivated fetal bovine serum, 200 μg/ml G418 (Sigma), 100 U/ml penicillin and 100 μg/ml streptomycin (Life Technologies). The cells were subcultured to ~85% confluence, harvested by trypsinization and stored in Tyrode's solution containing 0.5% bovine serum albumin (BSA) at 4°C.

2.2. Gene transfection

The constructs expressing the constitutively active bovine PI3K (caPI3K), pCMV6-p110α-mycC, and the dominant negative mouse PI3K (dnPI3K) in pcDNA3, pcDNA3-Δp110α-mycC, were kind gifts from Dr. L. Cantley [25]. The constitutively active mouse PKB in pECE (caPKB), and dominant negative bovine PKB in pCMV6 (dnPKB) were kind gifts from Dr. T. Franke and Dr. M. Greenberg [25,26]. The cDNA transfection procedures have been described in detail elsewhere [27]. Cells grown to ~80% confluence in 35 mm culture dishes with DMEM free of antibiotics were washed once with phosphate-buffered saline. Aliquots containing 2–3 μg of caPI3K, dnPI3K, caPKB, or dnPKB, plus 0.3 μg pπX-CD8 plasmid DNA were diluted into 100 μl DMEM and mixed well with 6 μl Plus reagent from the LipofectAMINE Plus reagent kit (Life Technologies) and incubated at room temperature (RT) for 15 min. The DNA-Plus reagent pre-complex was then added to 4 μl LipofectAMINE reagent in 100 μl of DMEM. The mixture was incubated at RT for 15 min and added to the cells in a dish containing fresh serum-free DMEM and swirled to distribute the complex uniformly, and incubated at 37°C under 5% CO_2 for 3 h. The cells were allowed to grow for 48 h before being harvested for analysis. Sham and blank control experiments were conducted in parallel. For electrophysiological experiments, the cells were harvested and incubated with 2 μl anti-CD8 Dynabead (Dynal ASA, Oslo, Norway) at RT for 15 min to label the transfected cells [27].

2.3. Whole-cell patch-clamp recording

Patch-clamp techniques have been described in detail elsewhere [27,28]. Currents were recorded with whole-cell voltage-clamp with an Axopatch-200B amplifier (Axon Instruments). Borosilicate glass electrodes had tip resistances of 1–3 MΩ when filled with (mM): 130 KCl, 1 $MgCl_2$, 5 Mg-ATP, 10 EGTA, 10 HEPES (pH 7.3). The extracellular solution contained (mM): 136 NaCl, 5.4 KCl, 1 $CaCl_2$, 1 $MgCl_2$, 10 glucose and 10 HEPES (pH 7.4). Experiments were conducted at 36 ± 1°C. Junction potentials were zeroed before formation of the membrane-pipette seal. Series resistance and capacitance were compensated and leak currents were subtracted.

WMN (PI3K inhibitor; Sigma Chemicals), bisindolylmaleimide (Bis; PKC inhibitor; Sigma Chemicals), and *N*-[2-(*p*-bromocinnamylamino) ethyl]-5-isoquinolinesulfonamide-2HCl (H89; PKA inhibitor; Biomol Research Labs, Plymouth Meeting, PA, USA) were dissolved in dimethyl sulfoxide as 1000× stock solutions and stored at −20°C, and the stock solutions were diluted to the desired concentrations right before the experiments.

2.4. Immunocytochemistry

The immunocytochemical procedures used have been previously described in detail [16,29]. In short, cells grown on coverslips were fixed with freshly prepared 1% paraformaldehyde, followed by permeabilization in 0.1% Triton X-100 and blocked in 1% BSA. Cells were then incubated overnight at 4°C with primary antibodies diluted in 1% BSA, followed by incubation with FITC- or TRITC-conjugated secondary antibodies at room temperature for 2 h. Rabbit polyclonal antibody against phospho-PKB (S473) was purchased from New England BioLabs (Beverly, MA, USA) and goat polyclonal anti-CD8 antibody was purchased from Santa Cruz (Santa Cruz, CA, USA). The specificity of the anti-phospho-PKB antibody has been tested in our previous studies [30]. Donkey anti-rabbit, FITC-conjugated and donkey anti-goat, TRITC-conjugated antibodies, purchased from Jackson Immuno-Research (Baltimore, MD, USA), were used as secondary antibodies. Non-specific staining by the secondary antibodies was excluded by the absence of staining in cells treated with the secondary antibodies alone. Coverslips were mounted onto glass slides with anti-fading mounting medium and were immediately examined under confocal laser scanning microscope equipment (model LSM 510; Zeiss). Excitation/emission wavelengths for FITC and TRITC were 488/512 and 543/576 nm, respectively and FITC (green) and TRITC (red) were excited separately to avoid bleed-through effects. The settings for laser scanning and image, such as laser power, pinhole, amplification factor and gain, were set optimal to avoid false positive or false negative stainings and for a given experiment, the settings were identical for all slides under examination. Each image represents an average from four consecutive slow-speed scannings. Density of staining by anti-phospho-PKB antibody was measured by the LSM 510 software suite and only positively stained cells were analyzed except for the cells in control group.

2.5. Data analysis

Group data are expressed as mean ± S.E.M. Paired or non-paired Student's *t*-tests were used for before-and-after or group comparisons as appropriate. A two-tailed $P < 0.05$ was taken to indicate a statistically significant difference. Non-linear least-square curve-fitting was performed with CLAMPFIT in pCLAMP 8.0 or Graphpad Prism.

3. Results

3.1. Effects of WMN on HERG currents (I_{HERG})

Currents were recorded in HEK293 cells stably expressing HERG with a two-step voltage protocol. The cell membrane was held at −80 mV, and stepped from −60 mV to +40 mV in 10 mV increments for 2.5 s to measure the step current and then returned to a constant potential at −50 mV for 2.5 s to measure the tail currents (Fig. 1A). The effects of the inhibitor of PI3K WMN were assessed following intracellular application. WMN (50 nM) was included in the pipette solution and dialyzed into the cytosol. Under our experimental conditions, 10 min was sufficient for complete dialysis. I_{HERG} was recorded right after membrane rupture and the same measurements were repeated every 5 min for a total of 20 min. The recordings made 15 min after membrane rupture were used to reflect the effects of WMN. As a control, cells were dialyzed and currents recorded in an identical fashion, but with WMN absent from the pipette solution. As illustrated in Fig. 1, WMN appeared to have two effects – a decrease in maximum conductance, along with a voltage shift tending to increase current at negative voltages. To ensure the suppression of I_{HERG} by WMN was not due to rundown of the current, we compared I_{HERG} recorded at various time points after membrane rupture. The data in Fig. 1C show that in the absence of WMN rundown of I_{HERG} was minimum (~5%) whilst in the presence of WMN I_{HERG} demonstrated a profound attenuation over a period of 15 min which coincided with the time course of dialysis of internal solution through a pipette under our experimental conditions. WMN did not alter the kinetics (time-dependent activation, inactivation and reactivation) of the current (data not shown).

Additional experiments were performed to ensure that the effects of WMN on I_{HERG} are not due to PKA and/or PKC activation. Cells were first bathed with H89 (1 μM) to inhibit PKA or Bis (100 nM) to inhibit PKC. Inhibitors were added to Tyrode's solution 20 min before patch-clamp recording with WMN (50 nM)-containing pipettes. Under these conditions, WMN produced qualitatively similar effects to those seen in experiments without H89 or Bis treatment. For example, I_{HERG} current density in the presence of H89 was 2.4 ± 0.6 pA/pF before and 3.4 ± 0.9 pA/pF ($P < 0.05$, $n = 6$) after WMN at −40 mV, and 51.7 ± 7.9 pA/pF before and 40.8 ± 7.3 pA/pF ($P < 0.05$) after WMN at 0 mV. In the presence of Bis, I_{HERG} densities were 2.7 ± 0.6 pA/pF before and 5.4 ± 1.3 pA/pF ($P < 0.05$, $n = 7$) after WMN at −40 mV, and 63.9 ± 10.1 pA/pF before and 55.3 ± 9.8 pA/pF ($P < 0.05$) after WMN at 0 mV. To validate the concentrations of H89 and

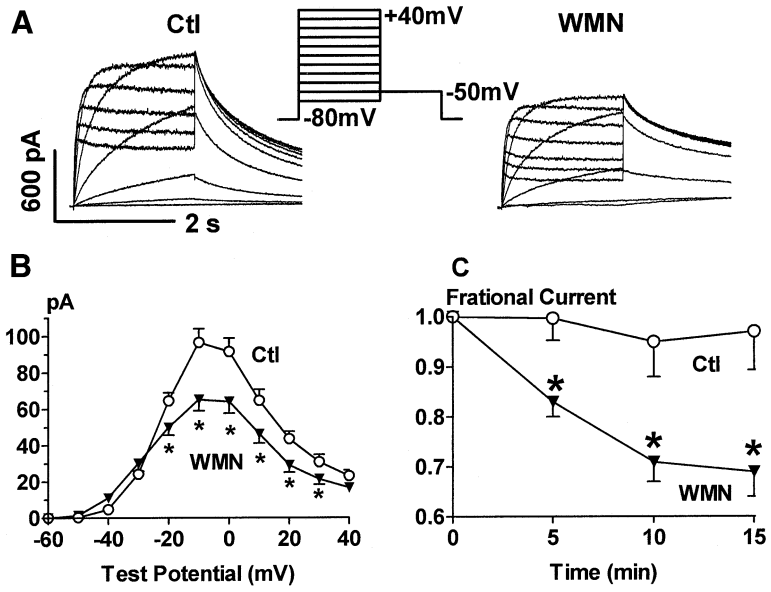

Fig. 1. Effects of WMN on I_{HERG} stably expressed in HEK293 cells. A: I_{HERG} recordings made immediately after membrane rupture with minimal dialysis, taken as baseline control data (Ctl), and 15 min after membrane rupture with complete dialysis through the pipette containing WMN (50 nM). I_{HERG} was elicited with the voltage protocol shown in the inset. The same voltage protocol is applied to the subsequent figures. B: I_{HERG} step current–voltage (I–V) relations. C: Changes of I_{HERG} amplitude at −10 mV with time after formation of whole cell configuration. Shown are data collected from recordings with pipettes without (Ctl, $n=8$) or with WMN ($n=8$). *$P<0.05$ WMN vs. control.

Bis used in our experiments, we conducted additional experiments with *Shaw*-like voltage-gated K^+ channel Kv4.3 expressed in HEK293 cells and we found that 1 μM H89 and 100 nM Bis completely reversed the effects produced by PKA and PKC stimulation caused by isoproterenol and phenylephrine, respectively (data not shown).

3.2. *Effects of constitutively active or dominant negative PI3K on I_{HERG}*

The results of the above experiments suggest that basal PI3K/PKB activation contributes to maintaining I_{HERG}/I_{Kr} function in the absence of external stimuli for PI3K/PKB activation. The data do not indicate whether the effects are due to PI3K activation, PKB activation or both. We began to address this issue by transiently transfecting caPI3K into HEK293 cells stably expressing HERG. I_{HERG} recorded in CD8 bead-labeled cells (indicating caPI3K transfection) was compared with I_{HERG} in untransfected cells or sham-treated counterparts. The data are presented in Fig. 2, where greater I_{HERG} density was seen at potentials negative to 0 mV in caPI3K-transfected cells relative to sham cells. For example, I_{HERG} density at −40 mV was 3.3 ± 0.4 pA/pF ($n=30$) for

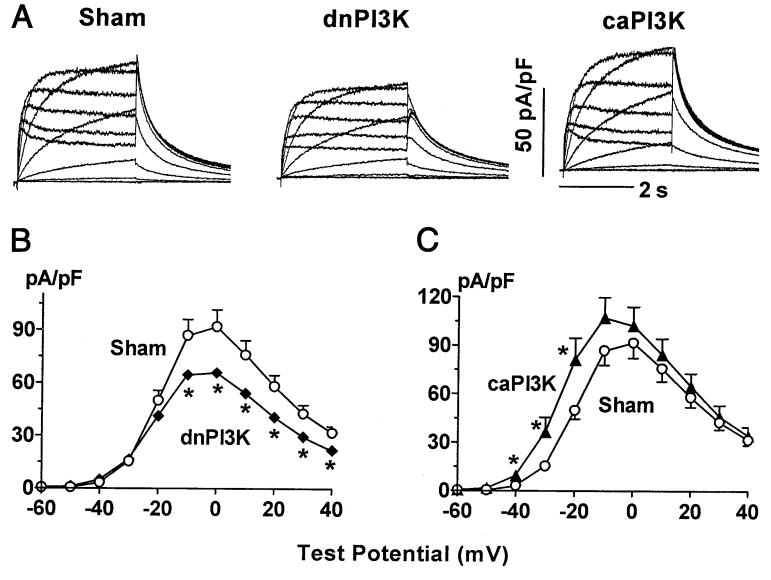

Fig. 2. I_{HERG} in cells transfected with caPI3K or dnPI3K. A: Typical examples of I_{HERG} traces presented as current density (pA/pF) for better group comparisons. For the sham group, the cells underwent the same transfection procedures as for dnPI3K and caPI3K groups, except that the plasmids were not included. B,C: I–V relationships averaged from 30 cells for sham, 25 cells for dnPI3K, and 28 cells for caPI3K group. *$P<0.05$ vs. sham.

sham control and 9.6 ± 3.6 pA/pF ($P < 0.05$, $n = 25$) for caPI3K (increased by ~2-fold), and at 0 mV was 91.9 ± 9.5 pA/pF for control and 102.4 ± 11.4 pA/pF for caPI3K (increased by ~10%, $P > 0.05$, unpaired t-test). At potentials positive to −10 mV, no appreciable differences between groups were observed. By contrast, the cells transfected with dnPI3K showed increased I_{HERG} only at potentials negative to −20 mV and moderate reduction of I_{HERG} was seen at potentials more positive than −20 mV. For example, I_{HERG} densities in dnPI3K-transfected cells was 7.1 ± 2.6 pA/pF (~2-fold larger than in the sham group, $P > 0.05$) at −40 mV, and was 79.1 ± 11.7 pA/pF (~25% smaller than in the sham group, $P > 0.05$) at 0 mV. The effects of dnPI3K are qualitatively comparable to those of WMN.

3.3. *Effects of constitutively active or dominant negative PKB on I_{HERG}*

To test the potential direct role of PKB, we performed experiments with transient transfection of caPKB or dnPKB in HERG-expressing HEK293 cells. Consistent with an important role for PKB, caPKB increased and dnPKB decreased I_{HERG}. Fig. 3 compares I_{HERG} in cells transfected with plasmids containing caPKB plus plasmids to cells with cDNAs expressing CD8 alone, as well as untreated control cells. In all cases, there were no significant differences in I_{HERG} between control and CD8-transfected cells. I_{HERG} density measured from caPKB cells was clearly greater than that of control or CD8-transfected cells at all voltages ranging from −40 to +40 mV, and there was a tendency towards greater differences at more positive potentials. For example, I_{HERG} density was 36%, 37% and 67% greater at −40 mV, 0 mV and +40 mV, respectively, in caPKB than in control cells (Fig. 3C). On the other hand, I_{HERG} was substantially smaller in dnPKB-transfected than in non-transfected or CD8-transfected cells at potentials positive to −20 mV, but was greater at potentials negative to this voltage (Fig. 3D–F). For instance, at 0 mV

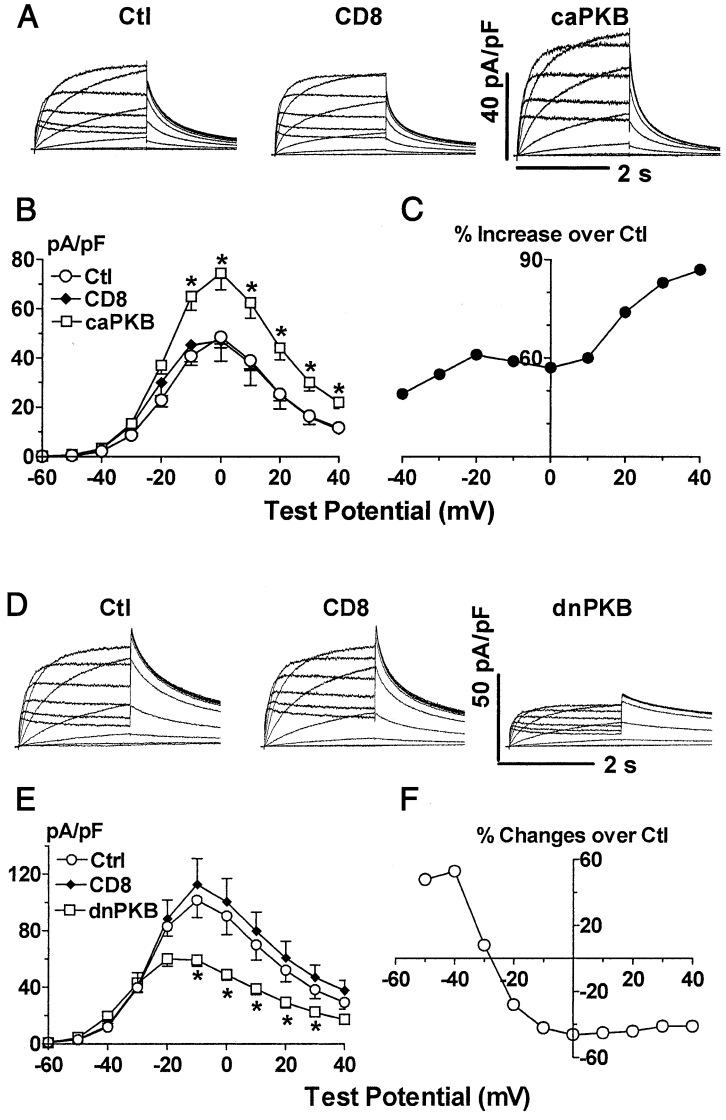

Fig. 3. I_{HERG} in HEK293 cells transfected with caPKB or dnPKB. A,D: Capacitance-normalized I_{HERG} traces (pA/pF) for better group comparisons. The HEK293 cells with stable expression of HERG were transiently transfected with plasmids containing cDNAs expressing CD8 alone (CD8 group) or with additional cDNA plasmids encoding caPKB or dnPKB. B,E: Mean I–V relationships. For caPKB experiments, $n = 19$ cell for Ctl, = 16 for CD8 alone, and = 23 for caPKB; for dnPKB experiments, $n = 20$ cell for Ctl, = 19 for CD8 alone, and = 19 for dnPKB. C,F: Percent difference of I_{HERG} density between caPKB or dnPKB and Ctl groups. *$P < 0.05$ vs. control (Ctl).

I_{HERG} density values were 90.4 ± 13.4 pA/pF ($n = 20$ cells) and 48.7 ± 3.9 pA/pF ($P < 0.05$, $n = 19$) in control and in dnPKB-transfected cells, respectively, whereas at −40 mV, the I_{HERG} density was 11.8 ± 1.6 pA/pF for control and 19.3 ± 5.0 pA/pF ($P < 0.05$) for dnPKB cells. These data indicated a 46% decrease at 0 mV and a 53% increase at −40 mV in the presence of dnPKB (Fig. 3F).

3.4. Immunocytochemical analysis of active PKB

To confirm that the effects of WMN in our experiments are associated with changes in PKB activity and that the cells transfected with caPKB or dnPKB indeed have increased or reduced PKB activity respectively, we performed immunostaining analyses of PKB activity using anti-phospho-PKB (S473) antibody. For WMN experiments, cells were preincubated with WMN (100 nM) in the culture medium for 30 min before being collected for immunostaining. As shown in Fig. 4A, the immunoreactivity was obviously weaker in WMN-treated than in control cells.

For caPKB/dnPKB experiments, double staining with anti-PKB antibody and anti-CD8 antibody was performed to distinguish the transfected from the non-transfected cells. The staining for phospho-PKB (green) was distributed in both the membrane and the cytoplasm, and CD8, a membrane protein co-transfected with caPKB as a marker for successful transfection, was stained red only to the plasma membrane. PKB staining was markedly more intense in cells also stained with CD8 than in cells with negative CD8 staining (non-transfected cells) in the same batch (Fig. 4B). The same was true when compared with the control cells that did not undergo the transfection procedures. In sharp contrast, the staining for phospho-PKB was nearly absent although the staining for CD8 was obvious in dnPKB-transfected cells.

The cells transfected with caPI3K showed a slightly higher intensity, while the cells transfected with dnPI3K showed a slightly lower intensity, of phospho-PKB staining than in their respective non-transfected cells or the control cells (Fig. 4B). The quantitative data are presented in Fig. 4C where the ratios of staining intensity in positively stained cells over non-stained control cells are shown.

4. Discussion

We demonstrated here that prevention of PI3K/PKB activation by pharmacological inhibition (WMN) or molecular inactivation (dnPI3K and dnPKB) significantly suppressed HERG function, whereas direct activation of PKB by introducing caPKB into the cell markedly enhanced HERG function. Inhibition of PKB activation by WMN or dnPI3K or dnPKB and increased activation of PKB with caPKB transfection were confirmed by immunocytochemistry with the use of the anti-phospho-PKB antibody. Our data clearly indicate that HERG K^+ channel function in HEK293 cells is enhanced by PKB activation and also provide the evidence for the first time that PKB phosphorylation participates in K^+ channel modulation.

WMN, used to inhibit PI3K activation and thereby the downstream PI3K-dependent PKB activation, produced remarkable depression (~30% reduction) of I_{HERG} stably expressed in HEK293 cells. The effects were observed under normal conditions in the absence of stimuli for PI3K/PKB activation. Coincidentally, dnPI3K caused virtually the same changes of I_{HERG} as WMN did: ~25% decrease in current density and ~5 mV shift of activation towards hyperpolarizing potentials. By comparison, direct inactivation of PKB by dnPKB produced a nearly doubled magnitude of effects on I_{HERG} as produced by WMN; dnPKB diminished I_{HERG} density by ~53% and shifted the $V_{1/2}$ by ~6 mV. In addition, while caPI3K produced only slight enhancement (~18%) of I_{HERG} function, caPKB strikingly increased I_{HERG} density (~52%). Correspondingly, caPI3K caused an only slight increase in the active form of PKB whereas caPKB boosted activation of PKB. Taken together these data allow us to reach the following conclusions: (1) the PI3K/PKB signaling pathway has regulatory effects on HERG K^+ channel function because inhibition of the pathway diminishes but activation of the pathway enhances I_{HERG}; (2) PI3K/PKB modulation of HERG is likely mediated by a direct effect of PKB but not PI3K phosphorylation because inhibition/activation of PKB produced far more pronounced effects on I_{HERG} compared with inhibition/activation of PI3K; (3) HERG is under tonic regulation of basal active PKB, or in other words, basal PKB activation is required for maintaining the normal physiological function of the HERG K^+ channel in HEK293 cells, because the effects of PKB inhibition on I_{HERG}, either by pharmacological blockade (WMN) or by molecular inactivation (dnPI3K and dnPKB), were seen in the absence of stimuli for PKB activation; and (4) the basal active PKB in HEK293 cells comes from both PI3K-dependent and PI3K-independent mechanisms. The PI3K-dependent activation PKB is WMN-sensitive, which can be prevented by treating the cells with WMN, while the PI3K-independent activation of PKB is WMN-insensitive. Introduction of dnPKB is expected to wipe out both PI3K-dependent and PI3K-independent activation of PKB. Indeed, our present study consistently showed that molecular inactivation of PKB by dnPKB produced some doubled magnitudes of I_{HERG} depression in comparison with the effects produced by WMN or dnPI3K. If the effects of WMN or dnPI3K on I_{HERG} arise from the PI3K-dependent activation of PKB, then the excess of effects produced by dnPKB over WMN or dnPI3K should represent PKB activation from PI3K-independent mechanisms.

The major finding of this study is that PKB has a tonic modulatory effect on I_{HERG}. Given the fact that dnPKB renders I_{HERG} density half of its size under normal conditions, it is expected that in the absence of basal PKB activation, I_{HERG} amplitude/density would be only 50% of its normal amplitude/density. It is therefore reasonable to conclude that the basal active PKB is required for maintaining the physiological function of I_{HERG} in HEK293 cells. Moreover, our data from caPKB experiments indicate that any further increase in PKB activation may further increase I_{HERG} beyond the basal conditions. Increased PKB activity has actually been noticed in a variety of physiological (such as growth stimulation, increased adrenergic tone, etc.) and diseased conditions (such as metabolic stress, oxidative challenge, ischemia, etc.) [3,4].

This finding may have some important pathophysiological implications. For example, it has long been known that the cardiac action potential duration (APD) is initially shortened in the early stage of acute myocardial ischemia and is subsequently prolonged in the late phase of ischemia, which is associated with the occurrence of different types of arrhythmias [31]. Coincidentally, PKB activities follow the same pattern of changes: a marked increase in the early phase followed

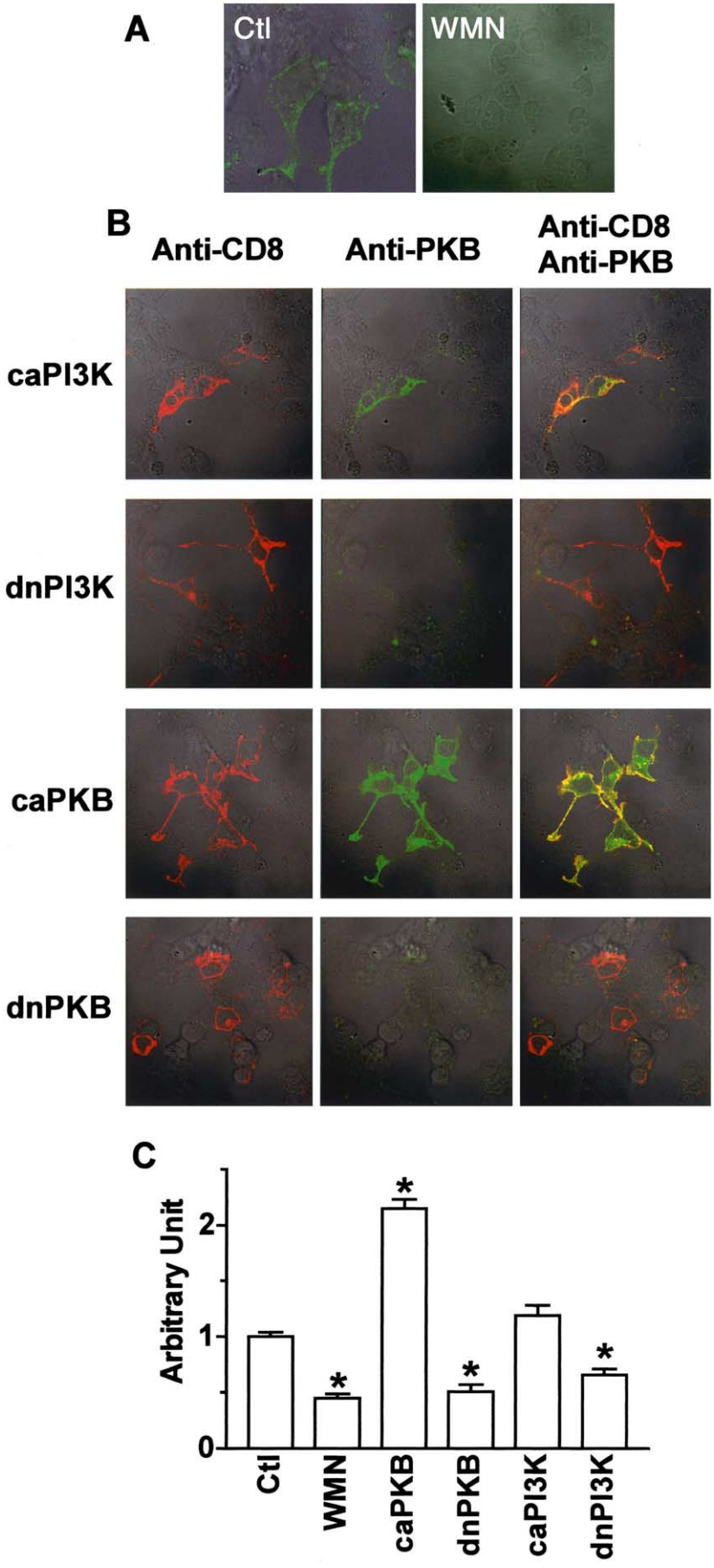
A
Ctl
WMN
B
Anti-CD8
Anti-PKB
Anti-CD8
Anti-PKB
caPI3K
dnPI3K
caPKB
dnPKB
C
Arbitrary Unit
0
1
2
*
*
*
*
*
Ctl
WMN
caPKB
dnPKB
caPI3K
dnPI3K

by an also marked drop in the late phase of ischemia [32]. Considering that the HERG-encoded K^+ current (the rapid component of delayed rectifier K^+ current or I_{Kr}) plays a critical role in determining cardiac APD [10,33], we can speculate that in the early phase of ischemia the increase in PKB activation enhances I_{Kr} which in turn accelerates the rate of cardiac repolarization or shortens APD, whereas in the late phase of ischemia when PKB activities are reduced I_{Kr} is correspondingly diminished which then leads to lengthening of APD. Also, cardiac APD was reported to be prolonged in myocytes isolated from animals with type I diabetes and slightly shortened in myocytes from type II diabetic animal model [34–36]. It is unclear whether this is associated with a decrease in PKB activation in type I diabetic subjects or an increase in type II diabetes.

The PI3K signaling pathway is involved in diverse cellular processes and some of these may be mediated by regulating ion channels. A recent work by Gamper et al. [9] demonstrated that insulin-like growth factor-1 (IGF-1) up-regulates several voltage-gated K^+ channels belonging to the *Shaker* subfamily including Kv1.1, Kv1.2 and Kv1.3 in HEK293 cells, and the effects were mediated by PI3K and its downstream targets 3-phosphoinositide-dependent protein kinase 1 and serum- and glucocorticoid-dependent kinase 1. Their data excluded the contribution of PKB to modulating *Shaker* K^+ channels. Enhancement of Cl^- channel by PI3K that contributes to volume regulation in rat hepatoma cells was reported by Feranchak et al. [8]. Using transient expression of wild-type, dominant negative, and constitutively active forms of PKB in cerebellar granule neurons, Blair et al. elegantly showed that IGF-1 partially mediates granule neuron survival via L-type Ca^{2+} channel activity and that PKB-dependent L-channel modulation is a necessary component because PKB mediates the IGF-1-induced potentiation of L-channel currents [6]. There have been no other previous studies on ion channel modulation by PKB. Our data represent the first evidence for the direct role of PKB in K^+ channel modulation.

PKA, PKC and PKB are all Ser/Thr protein kinases, which can phosphorylate their downstream effectors and alter the functional status of these downstream components. PKA and PKC both have been shown to modulate K^+ channels including HERG [19–23]. The minimum sequence motif required for optimal phosphorylation of peptide substrates by PKB is RXRXXS/T*, where X is any amino acid, and * is a bulky hydrophobic residue (phenylalanine or leucine) [3,4,17,18]. The sequence requirement for PKB phosphorylation is quite similar to that for PKC and distinct from that for PKA [18]. There are three putative PKA phosphorylation sites and one PKB favorite phosphorylation site (S890) in the C-terminal region, as well as one site (S331) in the N-terminal region, of the HERG sequence. Whether these sites are responsible for HERG modulation by PKB merits further studies with site-directed mutagenesis.

Acknowledgements: This work was supported by the Canadian Institutes of Health Research (CIHR), the Heart and Stroke Foundation of Quebec (HSFQ), and the Fonds de la Recherche de l'Institut de Cardiologie de Montréal. Z.W. is a research scholar of the Fonds de Recherche en Santé de Québec. H.H. and H.W. are research fellows of HSFC and CIHR, respectively. The authors thank XiaoFan Yang for her excellent technical support and Louis Villeneuve for his assistance in confocal microscope examination.

References

[1] Coffer, P.J. and Woodgett, J.R. (1991) Eur. J. Biochem. 201, 475–481.
[2] Jones, P.F., Jakubowicz, T., Pitossi, F.J., Maurer, F. and Hemmings, B.A. (1991) Proc. Natl. Acad. Sci. USA 88, 4171–4175.
[3] Chan, T.O., Rittenhouse, S.E. and Tsichlis, P.N. (1999) Annu. Rev. Biochem. 68, 965–1014.
[4] Vanhaesebroeck, B. and Alessi, D.R. (2000) Biochem. J. 346, 561–576.
[5] Wymann, M.P., Bulgarelli-Leva, G., Zvelebil, M.J., Pirola, L., Vanhaesebroeck, B., Waterfield, M.D. and Panayotou, G. (1996) Mol. Cell Biol. 16, 1722–1733.
[6] Blair, L.A., Bence-Hanulec, K.K., Mehta, S., Franke, T., Kaplan, D. and Marshall, J. (1999) J. Neurosci. 19, 1940–1951.
[7] Tokimasa, T., Ito, M., Simmons, M.A., Schneider, C.R., Tanaka, T., Nakano, T. and Akasu, T. (1995) Br. J. Pharmacol. 114, 489–495.
[8] Feranchak, A.P., Roman, R.M., Schwiebert, E.M. and Fitz, J.G. (1998) J. Biol. Chem. 273, 14906–14911.
[9] Gamper, N., Fillon, S., Huber, M., Feng, Y., Kobayashi, T., Cohen, P. and Lang, F. (2002) Pflugers Arch. 443, 625–634.
[10] Sanguinetti, M.C. (1999) Ann. NY Acad. Sci. 868, 406–413.
[11] Chiesa, N., Rosati, B., Arcangeli, A., Olivotto, M. and Wanke, E. (1997) J. Physiol. 501, 313–318.
[12] Crociani, O., Cherubini, A., Piccini, E., Polvani, S., Costa, L., Fontana, L., Hofmann, G., Rosati, B., Wanke, E., Olivotto, M. and Arcangeli, A. (2000) Mech. Dev. 95, 239–243.
[13] Rosati, B., Marchetti, P., Crociani, O., Lecchi, M., Lupi, R., Arcangeli, A., Olivotto, M. and Wanke, E. (2000) FASEB J. 14, 2601–2610.
[14] Arcangeli, A., Rosati, B., Cherubini, A., Crociani, O., Fontana, L., Ziller, C., Wanke, E. and Olivotto, M. (1997) Eur. J. Neurosci. 9, 2596–2604.
[15] Bianchi, L., Wible, B., Arcangeli, A., Taglialatela, M., Morra, F., Castaldo, P., Crociani, O., Rosati, B., Faravelli, L., Olivotto, M. and Wanke, E. (1998) Cancer Res. 58, 815–822.
[16] Wang, H., Zhang, Y., Cao, L., Han, H., Wang, J., Yang, B., Nattel, S. and Wang, Z. (2002) Cancer Res. 62, 4843–4848.
[17] Alessi, D.R., Caudwell, F.B., Andjelkovic, M., Hemmings, B.A. and Cohen, P. (1996) FEBS Lett. 399, 333–338.
[18] Obata, T., Yaffe, M.B., Leparc, G.G., Piro, E.T., Maegawa, H., Kashiwagi, A., Kikkawa, R. and Cantley, L.C. (2000) J. Biol. Chem. 275, 36108–36115.
[19] Kiehn, J., Karle, C., Thomas, D., Yao, X., Brachmann, J. and Kubler, W. (1998) J. Biol. Chem. 273, 25285–25291.
[20] Thomas, D., Zhang, W., Karle, C.A., Kathofer, S., Schols, W., Kubler, W. and Kiehn, J. (1999) J. Biol. Chem. 274, 27457–27462.
[21] Cui, J., Melman, Y., Palma, E., Fishman, G.I. and McDonald, T.V. (2000) Curr. Biol. 10, 671–674.
[22] Barros, F., Gomez-Varela, D., Viloria, C.G., Palomero, T., Giraldez, T. and de la Peña, P. (1998) J. Physiol. 511, 333–346.
[23] Jiang, M., Dun, W., Fan, J.S. and Tseng, G.N. (1999) J. Pharmacol. Exp. Ther. 291, 1324–1336.

←
Fig. 4. Immunocytochemical analysis of active PKB in HEK293 cells with anti-phospho-PKB (S473) antibody. A: Examples of confocal microscope images showing the cytoplasmic staining of the phosphorylated PKB (green) in HEK293 cells without (Control-Ctl, left) or with WMN (50 nM, right) treatment. B: Examples of double staining showing the membrane staining of CD8 (red) as a marker for successful transfection of varying constructs and the cytoplasmic staining of autophosphorylated (activated) PKB (green) and combination of the two (CD8+PKB, yellow), in HERG-expressing HEK293 cells transfected with caPI3K, dnPI3K, caPKB, or dnPKB. The phase-contrast images (Phase C) are superimposed for better views of the cell contour. C: Average density of green staining for phospho-PKB ($n=5$ independent experiments for caPI3K/dnPI3K and $n=4$ for caPKB/dnPKB) expressed as ratios over control. *$P<0.05$ vs. control.

[24] Zhou, Z., Gong, Q., Ye, B., Fan, Z., Makielski, J.C., Robertson, G.A. and January, C.T. (1998) Biophys. J. 74, 230–241.
[25] Franke, T.F., Kaplan, D.R., Cantley, L.C. and Toker, A. (1997) Science 275, 665–668.
[26] Dudek, H., Datta, S.R., Franke, T.F., Birnbaum, M.J., Yao, R., Cooper, G.M., Segal, R.A., Kaplan, D.R. and Greenberg, M.E. (1997) Science 275, 661–665.
[27] Wang, Z., Feng, J., Shi, H., Pond, A., Nerbonne, J.M. and Nattel, S. (1999) Circ. Res. 84, 551–561.
[28] Wang, H., Yang, B., Zhang, Y., Han, H., Wang, J., Shi, H. and Wang, Z. (2001) J. Biol. Chem. 276, 40811–40816.
[29] Wang, H., Han, H., Zhang, L., Shi, H., Schram, G., Nattel, S. and Wang, Z. (2001) Mol. Pharmacol. 59, 1029–1036.
[30] Han, H., Wang, H., Long, H., Nattel, S. and Wang, Z. (2001) J. Biol. Chem. 276, 26357–26364.
[31] Carmeliet, E. (1999) Physiol Rev. 79, 917–1017.
[32] Mockridge, J.W., Marber, M.S. and Heads, R.J. (2000) Biochem. Biophys. Res. Commun. 270, 947–952.
[33] Wang, Z., Fermini, B. and Nattel, S. (1994) Cardiovasc. Res. 28, 1540–1546.
[34] Casis, O., Gallego, M., Iriarte, M. and Sanchez-Chapula, J.A. (2000) Diabetologia 43, 101–109.
[35] Nordin, C., Gilat, E. and Aronson, R.S. (1985) Circ. Res. 57, 28–34.
[36] Shimoni, Y., Ewart, H.S. and Severson, D. (1998) J. Physiol. 507, 485–496.